RCS Simulation and Measurement Studies of Microwave Dipoles for Chaff Applications

Verandra Kumar[1], Prashant Vasistha[1, 2], and Ravindra Kumar[1]

[1]Defence Laboratory, DRDO, Jodhpur, 342011, INDIA
[2] Corresponding author: pvasistha@yahoo.com

Abstract. In this paper, monostatic RCS performance studies were carried out for metalized glass dipoles. RCS modelling and simulation has been carried out for array of dipoles which is followed by the RCS measurement in anechoic chamber at 3-8 GHz. Good agreement in the simulations and measurements has been observed which validates the comparison criteria and also the performance of dipoles for application as chaff material.

Keywords: Chaff, RCS, mutual coupling, polarization, dipole

1. Introduction

Thin metalized glass dipoles with very high aspect ratio are used as chaff materials for passive electronic countermeasure in modern warfare scenario. Chaff packs consist of electrically conducting thin filaments (diameter 25-30μ), cut to form dipoles of varying length that are resonant at specified frequencies of microwave radiations [1]. Chaff is a form of volumetric radar clutter designed to confuse the radar detection. These dipoles are dispensed into the atmosphere to generate the chaff cloud to deny radar acquisition, generate false targets, and to deny or disrupt radar tracking. Several chaff cloud models have been prepared in literature for the monostatic as well as bistatic RCS characterization as well as detailed information on chaff jamming technology [2-10]. RCS generated by chaff cloud is greatly affected by the mutual coupling, polarization and resonance. In chaff application, the early stage of interaction of aircraft with missile is very crucial. At early stage, the RCS is greatly influenced by the mutual copupling. The mutual coupling between the dipoles depends upon the relative orientation of the elements. The maximum coupling occurs when the dipoles are coplanarly distributed. Considering this aspect, the array model was prepared to study the mutual coupling effect between the dipoles.

A wide research is being carried out on microwave scatterring from wire strucrure. The current and field distribution model for wire type scatterers has been modelled by Richmond [11]. Mutual coupling effect in the dipole antenna array with the scattering characteristics has been carried out by several researchers [12-13].The RCS analysis of the linear array system has been modelled by Zhang [14], to optimize the arrangement of array so as to suppress the occurrence of the grating lobes. Further to the computational modelling, a hybrid approach for computing the RCS of wire type structures has been simulated by Seo [15] and the hybrid method was solved using Foldy Lax equation.

In this paper, the metalized glass dipoles are treated as the half wave dipoles with high aspect ratio and the dipole array was simulated using the element model and the array factor. Based on the prepared model, the mutual coupling effect of the array and the polarization effect on the array distribution has been investigated. The study of mutual coupling between dipoles is carried out analytically and then validated by the RCS measurement. The monostatic RCS measurement of the test coupons were also carried out for both co polar and cross polar configurations of antennas to evaluate the feasibility of the computational model.

2. The modelling of the chaff fibre array scattering

To carry out RCS measurement of dipoles, the arrangement of dipoles in array form is preferred over random distribution as it accounts for the conceptualization of the various factors such as mutual coupling and polarization and ease of measurement. The metalized glass dipole array model has been prepared for the measurement and simulation purpose. It is well known fact that the radiation field of an array arrangement can be represented as [16]

$$\vec{E}(\theta,\varphi) = \vec{E}_e(\theta,\varphi).E_a(\theta,\varphi) \quad (1)$$

where, $\vec{E}_e(\theta,\varphi)$and $E_a(\theta,\varphi)$ are the elements of the radiating fields of fibre element and array respectively in the spherical coordinate system. In the same manner, the RCS of the chaff fibre array model can be represented as the product of element RCS factor (σ_e) and array RCS factor (σ_A)[15]. These factors are represented as shown in Eq. (2)

$$\sigma_e = 4\pi r^2.\left|\frac{\vec{E}_e^s(\vec{k})}{\vec{E}_e^i(\vec{k})}\right|^2 \quad (2)$$

where, $\vec{E}_e^s$ is the scattered field from the target towards the radar receiver and $\vec{E}_e^i$is the incident field on the target. $\vec{k}$is the propagation vector of the field. The $\sigma_A$can be defined as shown in Eq. (3)

$$\sigma_A=\left|\sum_{m=0}^{M_x}\sum_{n=0}^{N_y} e^{j2k_0[sin(\theta)\cos(\varphi)mdx+sin(\theta)sin(\varphi)ndy]}\right|^2 \quad (3)$$

where, M_x and N_y represent the number of rows and columns of the array respectively, *dx* and *dy* represent the separation between the dipoles in the horizontal and vertical direction.

According to the above definition, the total RCS of the array can be written as shown in Eq. (4)

DOI: http://dx.doi.org/10.32452/IJAMT.2019.185189

$$\sigma(\theta,\varphi) = \sigma_e(\theta,\varphi).\ \sigma_A(\theta,\varphi) \quad (4)$$

where, θ and φ represents the orientation of fibre in the spherical coordinate system. The RCS of the dipole array has been broken down into two parts:

i) The element scattering factor and

ii) The array scattering factor.

The incident wave on dipole induces the current depending upon the wavelength and by integrating this current throughout the length the scattered field is calculated. The scattering field of a dipole element can be determined as [13] and can be shown as equation (5)

$$\vec{E}_\theta^s = \hat{x}\,.\,\theta\,\frac{i\eta}{4\lambda R_a}\,l^2 cos(\theta)cos(\varphi)\Gamma_0 e^{j\varphi_{mn}}\,\frac{e^{-jkr}}{r} \quad (5)$$

where, $R_a \approx 24.7(kl)^{2.4}$ is the dipole radiation resistance, Γ_0 as the backscattered reflection coefficient from the single element and l as the resonating length of the dipole i.e.λo/2. The element scattering factor is, thus, given by Eq. (6)

$$\sigma_e(\theta,\varphi) = 4\pi r^2 \left|\frac{\eta}{4\lambda R_a}\,l^2 cos^2(\theta)cos^2(\varphi)\Gamma_0\right|^2 \quad (6)$$

and the array scattering factor is shown in Eq. (7):

$$\sigma_A = \left|\sum_{m=0}^{M_x=M}\sum_{n=0}^{N_y=N} e^{j2k_0[\sin(\theta)\cos(\varphi)mdx+\sin(\theta)\sin(\varphi)ndy]}\right|^2 \quad (7)$$

Hence, the RCS of the 'M×N' dipole array is shown in Eq. (8):

$$\sigma(\theta,\varphi) = 4\pi r^2 \left|\frac{\eta_0}{4\lambda R_a}\,l^2 cos^2(\theta)cos^2(\varphi)\Gamma_0\right|^2 \times \left|\sum_{m=0}^{M_x=M}\sum_{n=0}^{N_y=N} e^{j2k_0[sin(\theta)\cos(\varphi)mdx+sin(\theta)sin(\varphi)ndy]}\right| \quad (8)$$

The validity of the proposed method can be demonstrated by comparing results obtained from Eq. (8) to those from a scattering formulation similar to the one described in [18]. From the method in [18], the total RCS of an array is defined as shown in Eq. (9)

$$\sigma(\theta,\varphi) = \left|\sum_{m=0}^{M_x}\sum_{n=0}^{N_y}\Gamma_{mn(\theta,\varphi)}e^{j\vec{k}.\vec{d}_{mn}}\right|^2 \quad (9)$$

where, $\Gamma_{mn(\theta,\varphi)}$ is the reflection coefficient of m^{th} element in the vicinity of n^{th} element. The derived expression (8) was used to simulate the RCS of the array formed of wire scatterers.

3. Simulation of '7x10' array of dipole length 5 cm

Theoretical simulation for a'7×10' array of linear dipoles of length 5 cm are carried out at 3 GHz using coding in MATLAB. Inter element spacing for this array is chosen 2λ (20 cm side by side) and λ (10 cm in collinear direction).

Figure 1 shows the variation of RCS with aspect angle of '7×10' array of 50mm dipole for horizontal polarization with horizontal separation of dipole as λ. Figure 2 shows the variation of RCS with aspect angle of '7 x10' array of 50mm dipole for vertical polarization with a vertical separation of dipole of 2λ. The placement of the array is carried out by rotating the target and antenna by 90^0. Figures 1 and 2 revealed that peak RCS is almost equal for both type of polarization as the numbers of elements remain same. Further, it has been observed that the numbers of grating

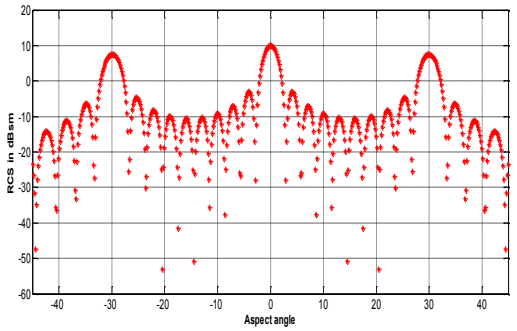

Fig. 1. RCS v/s azimuth cut simulation of '7x10 (M x N)' array of 50mm dipole for horizontal polarization at 3 GHz (Horizontal separation is λ)

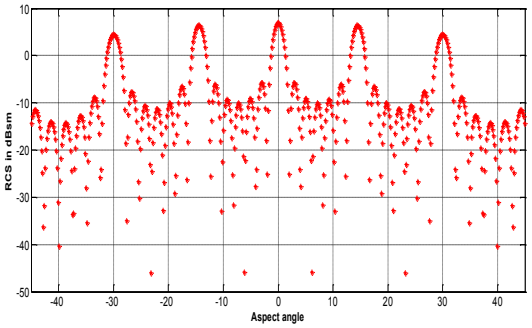

Fig. 2. RCS v/s azimuth cut simulation of ' 10x7 (M x N)' array of 50mm dipole for vertical polarization at 3 GHz (Vertical separation is 2 λ)

lobes were more in VV mode as compared to HH mode [19and 20] as in HH simulation the inter dipole spacing is λ whereas in VV simulation the inter dipole spacing is 2λ.It can be explained mathematically that the number of minima are 8 (N-2) as '7 x 10' (M x N) arrangement used for HH simulation whereas 5 (N-2) observed in VV measurement for '10x 7' (M x N) arrangement for the azimuth cut. In the following sections, preparation of test samples of metallized glass dipole array model and RCS measurement set up are described to compare the RCS simulation and measurement of dipole array model.

4. Measurements, results and discussion

4.1. Preparation of test coupons

The array model was generated to study the factors governing the RCS behaviour of the dipole. In preparation of array model, thermocol sheet (low dielectric constant) were used as a base material and the aluminium coated glass dipoleswere pasted on these thermocol sheets using radio transparent tape. Coupons were prepared for different dipole orientations (linear and random) and with different separation. These thermocol sheets are transparent to microwave and show very low RCS. The dipole length were taken as 28mm and 50 mm (so as to resonant at 5& 3 GHz respectively). The coupons were prepared by takingboth the fibers separately so as to make the comparison study. The number of elements were chosen as the quiet zone size constraints of the anechoic chamber. The details of the generated samples are as follows:

DOI: http://dx.doi.org/10.32452/IJAMT.2019.185189

I. Sample1: '5 x 8' array, dipole length as 28mm, with line by line separation 2λ, and collinear separation λ corresponding to 5 GHz.
II. Sample2: '5 x 8' array, dipole length as 28mm, with line by line separation λ, and collinear separation λ corresponding to 5 GHz.
III. Sample3: '5 x 8' array, dipole length as 28mm, random distribution with center to center separation in the vertical and horizontal direction as 2λ and λ respectively corresponding to 5 GHz.
IV. Sample4: '7 x 10' array, dipole length as 50mm, with line by line separation 2λ, and collinear separation λ corresponding to 3 GHz.
V. Sample5: '7 x 10' array, dipole length as 50mm, with line by line separation λ, and collinear separation λ corresponding to 3 GHz.

First two samples are shown in Figure 3 below to represent the schematic arrangement with horizontal and vertical separation.

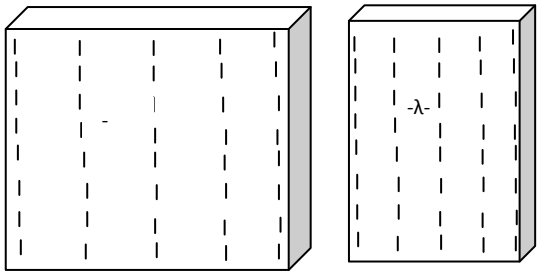

Fig. 3. 8×5 array linear distribution of 28mm length fiber with 2λ (Sample 1) and λ separation (Sample 2).

The different dipole distribution models were created to study the mutual coupling effect, polarization dependency on RCS and resonance effect of dipoles. RCS measurements were carried out for these samples for 3-8GHz in the anechoic chamber and measurement data were compared with the simulation of different distributions of dipole array.

4.2. Experimental setup for RCS measurement

The RCS measurements of the prepared coupons were carried out at the anechoic chamber. The Anechoic Chamber is of size 3m × 3m × 10m. The target-to-source distance is about 7m. The VNA based instrumentation is used for RCS and antenna pattern measurements. Broadband illumination horns covering the frequency range 3-8 GHz and 8-18 GHz with low side lobes for reduced coupling are used to transmit and receive. A target stand made of low-density foam is used for placement of the target. The instrumentation interfaces to a PC based controller over GPIB bus. Figure 4 shows the RCS measurement setup in the anechoic chamber at DL, Jodhpur.The gated CW radar VNA 8530C instrumentation was used for RCS measurement from 2-18 GHz.

Data is processed by background subtraction and calibration with respect to a known standard. In background subtraction, the frequency trace data of the chamber with the test target not present is subtracted from the corresponding frequency trace data with the test target present. This removes key clutter contributions including leakage between transmit and receive antennas, as well as chamber reflections

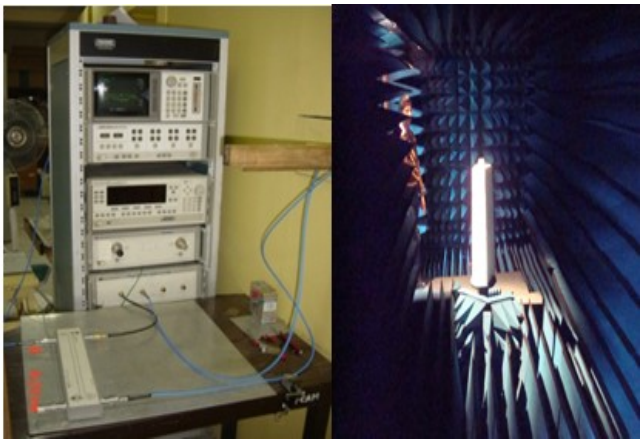

Fig.4 VNA instrumentation and anechoic chamber for RCS measurements

from the walls and absorbers. This data is then normalized to the data obtained by measuring a known calibration target like a precision cylinder or sphere. The normalization process removes any frequency response error of the instrumentation, and also permits the measurement result to be expressed directly in absolute dBsm. A 25 cm diameter calibration sphere is used for this purpose. The measurements were carried out for samples by taking different fiber compositions.

RCS versus frequency and RCS versus aspect angle measurement of the coupons prepared as per the details provided in section 3.1, were carried out to see the effect of mutual coupling and the polarization of antenna on the RCS response of the prepared array coupons. RCS versus frequency response and the RCS versus aspect angle pattern were generated and the various effects were determined. The performance of the metalized glass dipoles was measured and then validated using simulated data.

4.3. RCS versus frequency response

The figures 5-6 show the RCS versus frequency response comparison of the different compositions of the samples. It has been observed from the Figures 5-6 that increase in mutual coupling between the dipoles causes decrease in RCS of around 2-4 dBsm. Further reduction of around 5-8 dBsm has been observed for random distribution as it is because of the fact that random distribution causes return in orthogonal polarization.

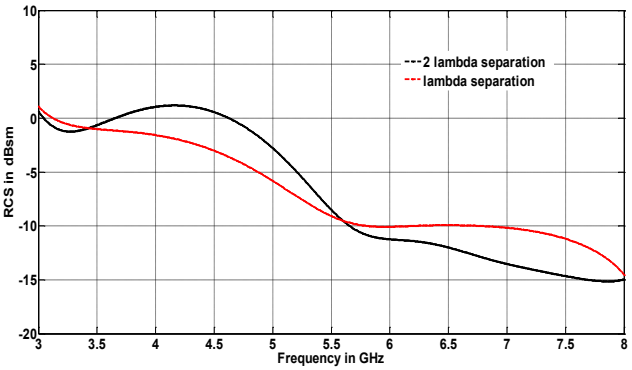

Fig. 5. RCS versus frequency comparison of metal coated glass fiber array with 2λ and λ separation (Sample 1 and Sample 2)

DOI: http://dx.doi.org/10.32452/IJAMT.2019.185189

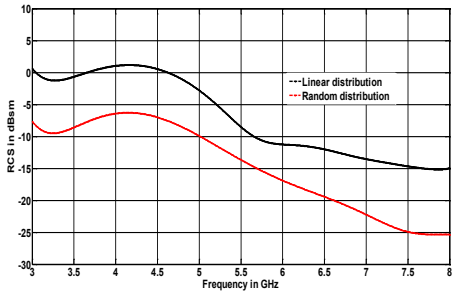

Fig. 6. RCS versus frequency comparison of metallic fiber array with linear and random distribution (Sample 1 and Sample 3))

Figures 7 and 8 show the effect of polarization of antenna in RCS measurement of array distribution. Co- and cross-polar response have been generated for both linear and random distribution and the comparison has been made using Sample 1 and Sample 3.

It has been observed from the Figures 7 and 8 that the difference in co- and cross- polar level for linear distribution model is around 35-40 dBsm whereas the difference is around 15-20 dBsm in random distribution model. This is due to the additional return in other polarization on the account of random distribution [21].

4.3. RCS versus aspect angle comparison

The theoretical modelling is done in MATLAB and the simulated results are compared with the measured pattern to validate the formulation. Figure 9 and 10 represent the RCS versus aspect angle pattern and the evaluation has been made on the basis of polarization and mutual coupling using the fabricated samples. It has been observed from the Figures 9 and 10 that the simulated RCS pattern is almost overlapping the pattern with measured RCS results with the same number of grating lobes and the number of minima between them.

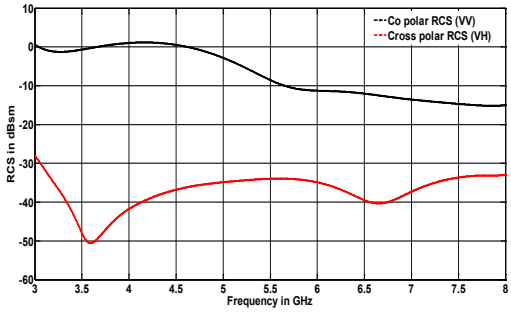

Fig. 7. RCS versus frequency comparison of VV and VH (Cross polar) measurement of the linear distributed array (Sample 1))

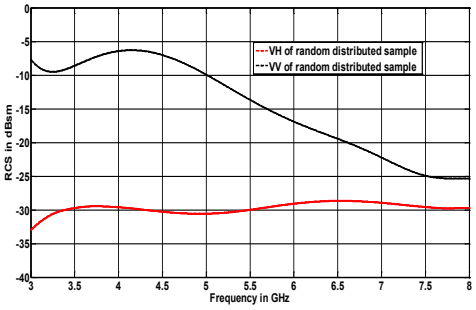

Fig. 8. RCS versus frequency comparison of VV and VH (Cross polar) measurement of random distributed array (Sample 3))

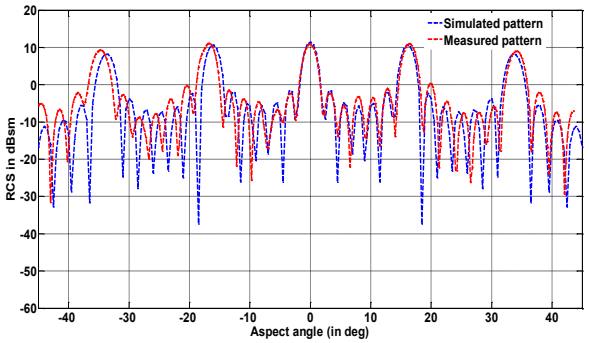

Fig. 9. RCS versus aspect angle comparison of simulation and measurement of metalized glass dipole array (‘10×7’) at 3 GHz for VV measurement .)

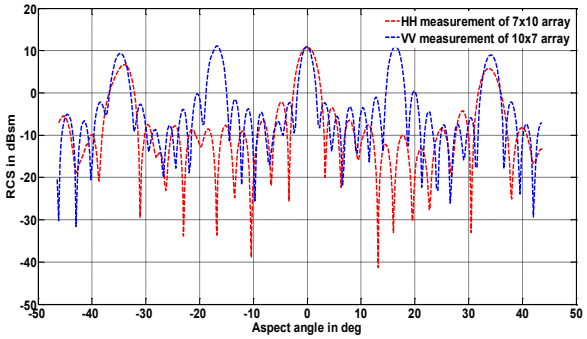

Fig. 10. RCS versus aspect angle comparison of HH and VV measurement at 3 GHz of the metalized glass dipole array (‘7×10’) model.

The elements and their orientation remain same for VV and HH polarization measurement for normal incidence. Hence the peak RCS is observed same for both the cases whereas the azimuth pattern cut changes for both type of polarization hence the difference in pattern is observed.

These measurements deal with the study of microwave interaction of metalized glass dipoles. The RCS versus frequency response as well as aspect angle pattern reveals that variation RCS is sturdily dependent on mutual coupling and polarization. The skin depth for aluminium is much lower than the coating thickness of aluminium on glass fibre. The interaction of microwave is only with the metallic part i.e. aluminium of metalized glass dipoles. It has been observed from RCS measurements that mutual coupling reduced the RCS by 2-4dBsm when inter element separation reduced from 2λ to λ. The mutual coupling effect has been modelled for three different configurations and it can be shown from simulation data that when the separation is greater than 2λ there will not be any mutual coupling between dipoles. The resonating effect was also observed in these measurements

The RCS versus aspect angle pattern is also generated for all the samples and a detailed comparison studies have been made between measurement and simulated data. The close agreement in the RCS measurement results shows the effectiveness of the theoretical model generated using the dipole antenna theory. The occurrence of grating lobes is observed in the pattern which may be useful in the specular reflection from other directions. The positions and number

DOI: http://dx.doi.org/10.32452/IJAMT.2019.185189

of grating lobes and number of side lobes in between grating lobes have been verified by measurement.

The different polarization measurements for the array have shown the RCS dependency of dipoles on polarization. Figure 10 shows the RCS measurement of dipole array in VV & HH polarization. The main peak value was found almost similar for both the polarization whereas the number of grating lobes have been reduced as the separation was λ for horizontal orientation as compared to 2 λ for vertical orientation. The number of side lobes in between main and grating lobe is observed as 8(N-2) for HH and 5(N-2) for VV polarization in measurement and simulation results. The cross polar return i.e. VH of random distributed array was observed more than that of linear distributed array. It reveals that the random distribution will lead to the return in the orthogonal polarization also. In actual application of these dipoles as a chaff cloud, the cross polar return will be significant as the distribution of dipoles will be 'more or less' random.

5. Conclusion

The RCS versus frequency response as well as aspect angle pattern show the RCS dependency on the mutual coupling between the dipoles and polarization state of the antennas. The simulated model has been validated based on RCS measurements with varying inter element spacing of the dipole, different polarization and mutual coupling. The slight discrepancy in the comparison may be accounted for due to preparation of test samples as the 100% equality of the samples cannot be guaranteed. The inter element spacing between the array elements reveals that the separation greater than 2λ will provide negligible mutual coupling. The polarization of antenna also significantly affects the RCS of array of dipoles. It is further observed from the RCS measurements that the dipoles may behave as a polarizer with random distribution as the significant cross polar return was observed for the randomly distributed dipoles.

Acknowledgement

The kind support received for fabrication and RCS measurement by MCDG group of Defence Laboratory, Jodhpur is gratefully acknowledged.

References

[1] B.C.F. Butters, Chaff, *Electronic Countermeasure, IEE Proceedings,* vol. 129, pp. 197-201, 1982.

[2] P. Z. Peebles, Bistatic radar cross section of chaff, *IEEE Transactions on Aerospace and Electronic Systems*, vol. 20, pp. 128-140, 1984.

[3] C. J. Palermo and L. H. Bauer, Bistatic scattering cross section of chaff dipoles with application to communication, *Proceedings of the IEE,* vol.53, pp.1119-1121, 1965.

[4] Xianli, Q. Teng, Chaff jamming effect to radar and math model building, *CIE International Conference on Radar*, pp. 16-20, 2006.

[5] S.W. Marcus, Dynamics and radar cross section density of chaff cloud, *IEEE Transaction on Aerospace and Electronic Systems*, vol. 40, pp. 93-102, 2004.

[6] K.G. Dedrick, A.R. Hessing, and G.L. Johnson, Bistatic radar scattering by randomly oriented wires, *IEEE Transactions on Antennas and Propogation*, vol. 26, pp. 420-426, 1978.

[7] Mingshan and W. Longtao, Research on the efficiency of the chaff jamming corridor, *IEEE Conference on Information Science and Control*, pp. 1673-1676, 2017.

[8] Cui and L. Shi, Identification of chaff interference based on polarization parameter measurement, *IEEE conference on Electronic Measurement and Instruments*, pp. 392-396, 2017.

[9] Zhong-fu and Li Jian-bing, Analysis of wideband characteristics and jamming technology of chaff cloud. *Proceedings of 3rd Asia-Pacific Conference on Antennas and Propagation*, pp. 1053-1057, 2014.

[10] Wang, The propagation properties of chaff clouds in atmosphere. Proceedings of 3rd Asia-Pacific Conference on Antennas and Propagation, pp. 783-788, 2014.

[11] J.H. Richmond, Scattering by an arbitrary array of parallel wire, *IEEE Transaction on Microwave Theory and Techniques*, vol. 13, 408-412, 1965.

[12] J.A.G. Malherbe, Analysis of a linear antenna array including the effect of mutual coupling, *IEEE Transaction on Education,* vol. 32,pp. 9-34, 1989.

[13] Bartsevich, Y. V. Bobkov, A. Al-Rifay, O.A. Yurtsev, Multi-element wire antenna array scattering characteristics numerical modelling, *6th International Conference on Antenna Theory and Techniques,* Ukraine, pp. 432-434, 2007.

[14] B. Lu and S. X. Gong, Analysis and synthesis of radar cross section of array antennas, *Progress In Electromagnetic Research*, vol. 16, pp.73-84, 2011.

[15] D.W. Seo, A hybrid method for computing the rcs of wire scatterers with an arbitrary orientation, *Progress In Electromagnetic Research B*, vol.23, pp. 55-68, 2010.

[16] Y. Huang and K. Boyle, *Antenna from Theory to Practice*, Wiley, pp. 191-200, 2008.

[17] S. Zhang, S.X. Gong, Y. Guan, and B. Lu, Optimized element positions for prescribed radar cross section pattern of linear dipole arrays, *International Journal of RF and Microwave Computer-Aided Engineering*, vol. 21, pp.622-628, 2011.

[18] B. Lu and S. X. Gong, A New method for determining the scattering of linear polarized element arrays, *Progress In Electromagnetic Research*, vol. 7, pp. 87-96, 2009.

[19] Y.D..M. Gong, *Theory of Antenna*, Xidian University Publishing Company,. Xi'an, 1997.

[20] C.A. Balanis, *Antenna Theory: Analysis and Design*. pp. 422-433, 2005.

[21] P. Pouliguen, Complete modelling of electromagnetic scattering by a cloud of dipoles, *Annales of Telecommunications*, vol. 48, pp. 305-318, 1963.

Biography of the authors

Verandra Kumar: He did his B Tech from MNIT, Jaipur in ECE during 2005-09. He joined DRDO in 2009 at Defence Laboratory, Jodhpur and currently working as Scientist C. His area of work includes RCS measurement and simulation of tagrets for stealth application as well as Dynamic RCS modelling, simulation and measurements of decoys currently being used by IAF and IN.

Prashant Vasistha: He did his PhD from Department of Electronics Engineering, IIT(BHU), Varanasi. He joined DRDO in 1998 at Defence Laboratory, Jodhpur. He has been working in the area of radar cross section (RCS) studies and RCS measurement technologies for combat systems. He has an experience of 18 years in the area of radar camouflage and electronic counter measure decoys.

Ravindra Kumar: He did his BE from IIT Roorkee in 1983 and M Tech from IIT Mumbai in 1987. He joined DRDO in 1983 at DL, Jodhpur. He has an R&D experience of 35 years in the area of desert warfare scenraio management, Phase change materials, water purifications systems and design, development and testing of electronic countermeasures.

DOI: http://dx.doi.org/10.32452/IJAMT.2019.185189